Modeling of Nonlinear Interference in the Same-Wavelength Bidirectional Coherent Fiber Communication Systems

Yuan Li ⓘ, Chengcheng Wu ⓘ, Peili He ⓘ, Wei Li ⓘ, Shaohua Yu ⓘ, Ming Luo ⓘ, Zhongshuai Feng ⓘ, Muyang Mei ⓘ, *Student Member, IEEE*, Qianggao Hu, Liyan Huang ⓘ, and Haitao Li ⓘ

Abstract—A detailed theoretical study is conducted on the nonlinear interference in the same-wavelength bidirectional coherent optical fiber communication systems. The Gaussian noise (GN) model used to evaluate nonlinear interference (NLI) in unidirectional systems is applied and extended to bidirectional transmission scenarios. The extended NLI model shows that in a bidirectional transmission communication system, the backward signal almost does not introduce additional nonlinear crosstalk to the forward signal due to the strong walk-off effect between forward and backward transmitted signals. Specifically, the ratio of the nonlinear crosstalk introduced by the forward and backward signals is about 21 dB, which means that the traditional GN model is also applicable in the bidirectional scenario. This conclusion is validated on the platform of a same-wavelength bidirectional coherent optical communication system based on Optisystem software.

Index Terms—Coherent fiber communication, GN model, nonlinear interference, optical transmission, same-wavelength bidirectional scheme.

I. INTRODUCTION

OPTICAL fiber communication technologies have developed to the point that almost all orthogonal dimensions of the optical field have been utilized for capacity expansion [1], [2], [3]. The transmission capacity of current optical fiber communication systems is approaching the limit set by the nonlinear Shannon limit, which makes further improvement challenging [4], [5]. However, in recent years, with the rapid development of various high-tech technologies, global data traffic has shown an explosive growth trend, which is continuously putting pressure on the current optical fiber communication systems. New capacity expansion solutions for optical fiber communication systems are urgently needed.

Similar to the full-duplex technologies in wireless communication systems, ideally, the same-wavelength bidirectional (SWB) coherent fiber communication scheme could double the transmission capacity of existing optical fiber communication systems [6], [7]. Therefore, it has great potential in fiber capacity expansion, which might allow the transmission capacity of single-mode fiber to break through the limit of 100 Tbit/s. However, the practical application of this scheme will face with two major kinds of crosstalk, including Fresnel reflection and Raleigh scattering noise [8], [9]. The elimination of Fresnel reflection crosstalk can be achieved by using mature digital signal processing (DSP) techniques or reducing the use of active fiber connectors through fusion splicing [10], [11], [12]. For Rayleigh scattering noise, its transmission and accumulation processes have inherent differences compared to the signal light. This results in a power difference between the signal light and the Rayleigh scattered light at the receiving end. Therefore, by adjusting the distributed gain in the fiber link, this power difference can be enlarged, consequently effectively suppressing the impact of Rayleigh scattering noise [13].

In addition to the aforementioned crosstalk issues, the behavior of nonlinear interference (NLI) in bidirectional systems is also worth exploring. In optical fiber communication systems, when the transmitted optical power reaches a certain level, the quality of the signal is severely affected by the Kerr nonlinearity of the fiber [14]. In a unidirectional coherent optical communication system, if the input optical power is doubled, the intensity of nonlinear crosstalk in the fiber will increase by a factor of 2^3 [15]. For the bidirectional coherent optical communication system depicted in Fig. 1, the total optical power transmitted in the fiber is doubled due to the addition of signals from both ends. This meets the power requirement for generating significant nonlinear effects. However, it remains to be determined whether strong nonlinear interactions will be introduced from the backward-propagating signal lights. Further theoretical derivation and analysis are needed to investigate this. Therefore, it is necessary to quantitatively model the nonlinear interference in this scenario.

Yuan Li is with the School of Computer Science, Central China Normal University, Wuhan 430079, China (e-mail: yuanli@ccnu.edu.cn).

Chengcheng Wu, Peili He, Wei Li, Zhongshuai Feng, and Muyang Mei are with the Wuhan National Laboratory for Optoelectronic, Huazhong University of Science and Technology, Wuhan 430074, China (e-mail: cc_wu@hust.edu.cn; m202173338@hust.edu.cn; weilee@hust.edu.cn; zsfeng@hust.edu.cn; muyangmei@hust.edu.cn).

Shaohua Yu is with Peng Cheng Laboratory, Shenzhen 518000, China (e-mail: yush@cae.cn).

Ming Luo is with the State Key Laboratory of Optical Communication Technologies and Networks, China Information Communication Technologies Group Corporation, Wuhan 430074, China (e-mail: mluo@wri.com.cn).

Qianggao Hu, Liyan Huang, and Haitao Li are with Accelink Technologies Company, Ltd., Wuhan 430205, China (e-mail: qianggao.hu@accelink.com; liyan.huang@accelink.com; haitao.li@accelink.com).

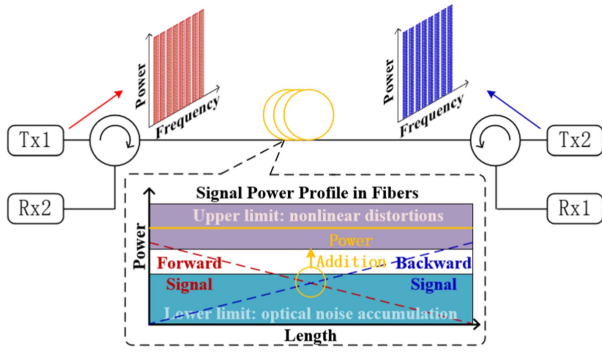Digital Object Identifier 10.1109/JPHOT.2023.3317948

Fig. 1. Power evolution schematic diagram of the signal light in a same-wavelength bidirectional coherent optical communication system.

Indeed, the modeling of NLI in optical fiber communication systems is of significant importance. On the one hand, it allows for the evaluation of the system's quality under the influence of nonlinear effect [16], [17]. On the other hand, it provides guidance for optimizing the design of system parameters [18], [19]. To address this need, scholars worldwide have proposed numerous nonlinear models for optical fiber communication systems [15], [20], [21]. Among these models, the GN model proposed by P. Poggiolini has gained significant attention [22], [23], [24]. For the SWB schemes we are concerned with, the existing form of the GN model cannot be directly used to evaluate the intensity of its nonlinear interference.

This article mainly focuses on the theoretical research of NLI in SWB coherent optical communication systems. Firstly, to address the limitation of the existing GN model that is only applicable to unidirectional transmission systems, we start with the nonlinear Schrodinger equation (NLSE) in the bidirectional scenario. By adopting the assumptions and derivation approach of the traditional GN model, we present a GN model specifically designed for the bidirectional transmission scenario. After analyzing and discussing this model, we found that in a SWB system, due to the strong walk-off effect between the forward and backward transmitted signals, the backward signal hardly generates additional nonlinear crosstalk on the forward signal. The ratio of crosstalk contributions between the two directions is approximately 21 dB, indicating that the system's tolerance to nonlinear effects is almost identical to that of traditional unidirectional systems. Therefore, the traditional GN model is also applicable in this scenario. Finally, we built a simulation platform for SWB coherent optical communication using Optisystem software. We considered transmission distances of 80/100/120 km and compared the received error vector magnitude (EVM) of the signal in both unidirectional and bidirectional transmission systems.

II. DERIVATION OF THE NONLINEAR INTERFERENCE MODEL

As mentioned earlier, the GN model is an effective tool for accurately assessing the nonlinear interference caused by the Kerr effect in optical fiber communication systems. However, its current form is only applicable to unidirectional transmission scenarios. Therefore, in this section, we will focus on extending its application to same-wavelength bidirectional scenarios and

use it to evaluate the nonlinear interference introduced by the backward signal in this system.

In this context, we continue to apply the three assumptions of the signal model as derived in the GN model [25]. Firstly, we assume that the signal possesses the statistical properties of a stationary Gaussian random process. This assumption holds approximately when the accumulated dispersion in the system is sufficiently large. Secondly, we assume that the signal model exhibits periodicity, with a period equal to an integer multiple of the symbol baud rate. This assumption is not restrictive since we can consider the period of practical signals is infinite. Thirdly, we assume that the average power spectral density of the signal model is shaped by the transmit spectrum. Under the three assumptions, the representations of the signal model in time-domain and frequency-domain at $z = 0$ can be expressed as follows, respectively:

$$E\left(0, t\right) = \sqrt{f_0 G_{Tx/Rx}\left(n f_0\right)} \sum_{n=-\infty}^{+\infty} \xi_n e^{j2\pi n f_0 t} \quad (1)$$

$$E\left(0, f\right) = \sqrt{f_0 G_{Tx/Rx}\left(f\right)} \sum_{n=-\infty}^{+\infty} \xi_n \delta\left(f - n f_0\right) \quad (2)$$

Where $f_0 = 1/T$ represents the frequency of the periodic signal. $G_{Tx/Rx}$ represents the power spectral density of the transmitted/received signal. ξ_n is a complex Gaussian random variable with zero mean and unit variance.

Taking the modulus square of (2) and integrating over frequency yields the corresponding power value, as shown in (3):

$$P_{Tx/Rx} = f_0 \sum_{n=-\infty}^{+\infty} G_{Tx/Rx}\left(n f_0\right) \left|\xi_n\right|^2 \quad (3)$$

We will still start with the NLSE equation to attempt to obtain the nonlinear interference model in SWB coherent optical communication systems. In this scenario, the NLSE can be expressed as follows:

$$\begin{cases} \frac{\partial}{\partial z} E_+\left(z, f\right) = -j\beta\left(f\right) E_+\left(z, f\right) + \left[-\alpha + g\left(z\right)\right] \\ \qquad E_+\left(z, f\right) + Q_{NLI,+} \\ \frac{\partial}{\partial z} E_-\left(z, f\right) = +j\beta\left(f\right) E_-\left(z, f\right) - \left[-\alpha + g\left(z\right)\right] \\ \qquad E_-\left(z, f\right) + Q_{NLI,-} \end{cases} \quad (4)$$

Wher E_+ and E_- represent the signal optical fields for forward and backward transmission, respectively. $\beta\left(f\right)$ is the corresponding propagation constant. α and $g\left(z\right)$ represent the fiber loss and distributed gain. $Q_{NLI,\pm}$ are the Kerr terms, which can be stated as:

$$\begin{cases} Q_{NLI,+}\left(z, f\right) = -j\gamma\left[E_+\left(z, f\right) * E_+^*\left(z, f\right) + E_-\left(z, f\right) \right. \\ \qquad \left. * E_-^*\left(z, f\right)\right] * E_+\left(z, f\right) \\ Q_{NLI,-}\left(z, f\right) = +j\gamma\left[E_+\left(z, f\right) * E_+^*\left(z, f\right) + E_-\left(z, f\right) \right. \\ \qquad \left. * E_-^*\left(z, f\right)\right] * E_-\left(z, f\right) \end{cases}$$

$$\tag{5}$$

Where the symbol '$*$' represents the convolution operation. See Appendix for the derivation process.

Directly solving (5) is challenging, so in this case, we first examine its characteristics near the input fiber end. Considering that $Q_{NLI,+}$ and $Q_{NLI,-}$ have cyclic symmetry, we only need

to derive the solution for $Q_{NLI,+}$ in the following discussion. At $z = 0$, substituting the signal model described by (2) into (5) yields:

$$Q_{NLI,+}(0, f) = -j\gamma f_0^{\frac{3}{2}} \times$$

$$\left\{ \begin{array}{l} \sum_{i=-\infty}^{+\infty} \delta(f - if_0) \sum_{m,n,k \in A_i} \\ \times \sqrt{G_{Tx,+}(mf_0) G_{Tx,+}(nf_0) G_{Tx,+}(kf_0)} \xi_{m,+} \xi_{n,+}^* \xi_{k,+} + \\ \sum_{i=-\infty}^{+\infty} \delta(f - if_0) \sum_{m,n,k \in A_i} \\ \times \sqrt{G_{Rx,-}(mf_0) G_{Rx,-}(nf_0) G_{Tx,+}(kf_0)} \xi_{m,-} \xi_{n,-}^* \xi_{k,+} \end{array} \right\}$$
(6)

Where A_i represents a collection of arrays, which is defined as:

$$A_i \equiv \{(m, n, k) : m - n + k = i\} \tag{7}$$

For further convenience, we divide A_i into two subsets, X_i and A_i, defined as:

$$X_i \equiv \{(m, n, k) : [m - n + k = i] \text{ and } [m = n \text{ or } k = n]\} \tag{8}$$

$$\tilde{A}_i = A_i - X_i \tag{9}$$

Based on this, we can also divide $Q_{NLI,+}(0, f)$ into two parts as follows:

$$Q_{NLI,+}(0, f) = Q_{NLI,+,X_i}(0, f) + Q_{NLI,+,\tilde{A}_i}(0, f) \tag{10}$$

Under the subset X_i, combining the signal model given by (1) and (2), we can further simplify $Q_{NLI,+.X_i}(0, f)$ as follows:

$$Q_{NLI,+,X_i}(0, f) = -j\gamma f_0^{\frac{3}{2}}$$

$$\times \left\{ \begin{array}{l} 2 \times \sum_{i=-\infty}^{+\infty} \delta(f - if_0) \sqrt{G_{Tx,+}(if_0)} \xi_{i,+} \\ \times \sum_{n=-\infty}^{+\infty} G_{Tx,+}(nf_0) |\xi_{n,+}|^2 + \\ \sum_{i=-\infty}^{+\infty} \delta(f - if_0) \sqrt{G_{Tx,+}(if_0)} \xi_{i,+} \\ \times \sum_{n=-\infty}^{+\infty} G_{Rx,-}(nf_0) |\xi_{n,-}|^2 \end{array} \right\}$$

$$= -j\gamma \sqrt{f_0} \left(2P_{Tx,+} + P_{Rx,-} \right) \sum_{i=-\infty}^{+\infty} \delta(f - if_0)$$

$$\times \sqrt{G_{Tx,+}(if_0)}$$

$$= -j\gamma \left(2P_{Tx,+} + P_{Rx,-} \right) E_+(0, f) \tag{11}$$

The above result indicates that the role of $Q_{NLI,+.X_i}(0, f)$ is to introduce a fixed nonlinear phase shift that is only dependent on the power, and the contributions of the forward and backward signals to this part are in a ratio of 2:1.

To extrapolate the result of (11) to any position z, we can get the following expression:

$$Q_{NLI,+,X_i}(z, f) = -j\gamma \{P_{Tx}[2p_+(z) + p_-(z)]\} E_+(z, f) \tag{12}$$

Where $p_+(z)$ and $p_-(z)$ are the normalized signal power, and they can be defined as follows:

$$\begin{cases} p_+(z) = \exp\left(2\int_0^z [-\alpha + g(z)] dz\right) \\ p_-(z) = \exp\left(2\int_0^{L-z} [-\alpha + g(z)] dz\right) \end{cases} \tag{13}$$

At this point, we have obtained the solution for $Q_{NLI,+.X_i}(z, f)$ in subset X_i. Substituting (10) and (12) into (4), we have:

$$\frac{\partial}{\partial z} E_+(z, f) = \left\{ \begin{array}{c} -j\beta(f) - \alpha + g(z) \\ -j\gamma P_{Tx} [2p_+(z) + p_-(z)] \end{array} \right\}$$

$$\times E_+(z, f) + Q_{NLI,\tilde{A}_i,+}(z, f) \tag{14}$$

After integrating both sides of the equation, it is found that the solution can be split into two parts as follows:

$$\begin{cases} E_+(z, f) = E_{LIN,+}(z, f) + E_{NLI,+}(z, f) \\ E_{LIN,+}(z, f) = e^{\Gamma(z,f)} E_+(0, f) \\ E_{NLI,+}(z, f) = e^{\Gamma(z,f)} \int_0^z e^{-\Gamma(\sigma,f)} Q_{NLI,+,\tilde{A}_i}(\sigma, f) d\sigma \end{cases} \tag{15}$$

Where $E_{LIN,+}$ represents the linear solution part of the equation, which characterizes the effects of dispersion, loss, gain and the fixed nonlinear phase shift. $E_{NLI,+}$ represents the nonlinear solution part, which represents the influence of the nonlinear Kerr effect in subset $\tilde{A}_i$. The definition of $\Gamma(z, f)$ is given by (16):

$$\Gamma(z, f) = -j\beta(f) z + \int_0^z [-\alpha + g_+(\sigma)] d\sigma$$

$$- \int_0^z j\gamma P_{Tx} [2p_+(\sigma) + p_-(\sigma)] d\sigma \tag{16}$$

It is worth noting that in coherent optical communication systems, the fixed phase shift introduced by nonlinear effects can be easily compensated through receiver-side DSP processing techniques, which does not affect signal reception. Therefore, $E_{NLI,+}$ is the true source of nonlinear interference, whose presence directly leads to degradation in signal quality.

From (15), it appears that in order to obtain the nonlinear interference term $E_{NLI,+}$, we need to know the form of $Q_{NLI,+,\tilde{A}_i}$. However, $Q_{NLI,+,\tilde{A}_i}$ is strongly related to $E_+(z, f)$ (or $E_{NLI,+}$), which creates a circular dependency in the solution process. To avoid this, we make the assumption that the nonlinear interference is present in a perturbative form relative to the linear part of the optical field. Therefore, we have:

$$E_+(z, f) \approx E_{LIN,+}(z, f) = e^{\Gamma(z,f)} E_+(0, f) \tag{17}$$

By substituting (17) and (2) into (5) and rearranging, we obtain:

$$Q_{NLI,+,\tilde{A}_i}(z, f) = -j\gamma f_0^{\frac{3}{2}}$$

$$\times \left\{ \begin{array}{l} \sum_{i=-\infty}^{+\infty} \delta(f - if_0) \sum_{m,n,k \in \tilde{A}_i} \\ \times \sqrt{G_{Tx,+}(mf_0) G_{Tx,+}(nf_0) G_{Tx,+}(kf_0)} \times \\ \xi_{m,+} \xi_{n,+}^* \xi_{k,+} p_+(z)^{\frac{3}{2}} e^{-j[\beta(mf_0) - \beta(nf_0) + \beta(kf_0)]z} + \\ \sum_{i=-\infty}^{+\infty} \delta(f - if_0) \sum_{m,n,k \in \tilde{A}_i} \\ \times \sqrt{G_{Rx,-}(mf_0) G_{Rx,-}(nf_0) G_{Tx,+}(kf_0)} \times \\ \xi_{m,-} \xi_{n,-}^* \xi_{k,+} p_+(z)^{-\frac{1}{2}} e^{-j[-\beta(mf_0) + \beta(nf_0) + \beta(kf_0)]z} \end{array} \right\}$$
(18)

In the above equation, the fixed nonlinear phase shift term is omitted for simplicity of expression, which does not have any impact on the final result.

By substituting (18) into (15), we can obtain the electric field representation of the nonlinear interference.

After simplification, its form is given as follows:

$$E_{NLI,+}(z,f)$$

$$= -j\gamma f_0^{\frac{3}{2}}\sqrt{p_+(z)}\sum_{i=-\infty}^{+\infty}\delta(f-if_0)\left(\mu_i^{(1)}+\mu_i^{(2)}\right) \quad (19)$$

Where:

$$\mu_i^{(1)} = \sum_{m,n,k\in\tilde{A}_i}\sqrt{G_{Tx,+}(mf_0)G_{Tx,+}(nf_0)G_{Tx,+}(kf_0)}$$

$$\times \xi_{m,+}\xi_{n,+}^*\xi_{k,+}$$

$$\times \int_0^z p_+(\sigma)e^{j\{\beta[(m-n+k)f_0]-\beta(mf_0)+\beta(nf_0)-\beta(kf_0)\}\sigma}d\sigma$$

$$(20)$$

$$\mu_i^{(2)} = \sum_{m,n,k\in\tilde{A}_i}\sqrt{G_{Rx,-}(mf_0)G_{Rx,-}(nf_0)G_{Tx,+}(kf_0)}$$

$$\times \xi_{m,-}\xi_{n,-}^*\xi_{k,+}$$

$$\times \int_0^z \frac{1}{p_+(\sigma)}e^{j\{\beta[(m-n+k)f_0]+\beta(mf_0)-\beta(nf_0)-\beta(kf_0)\}\sigma}d\sigma$$

$$(21)$$

We are more interested in the average power of the nonlinear crosstalk rather than its electric field form. Therefore, we obtain its average power spectral density by taking the squared modulus of (19) and then performing the averaging operation.

$$G_{NLI}(f) = \mathrm{E}\left\{|E_{NLI,+}(z,f)|^2\right\}$$

$$= \mathrm{E}\left\{E_{NLI,+}(z,f)\times E_{NLI,+}^*(z,f)\right\} \quad (22)$$

Where E{} represents the averaging operator, and the superscript $*$ denotes the complex conjugate.

Note that $E_{NLI,+}$ is composed of numerous independent zero-mean random variables. Therefore, not all parts contribute to its expectation. This can be mathematically expressed as follows:

$$\mathrm{E}\left\{\xi_{m,p}\xi_{n,q}^*\right\} = \begin{cases} 1, m=n\,\mathrm{and}\,p=q \\ 0, \mathrm{others} \end{cases} \quad (23)$$

During the expansion process in (22), the following expectation operations are involved:

$$\begin{bmatrix} \mathrm{E}\left\{\xi_{m,+}\xi_{n,+}^*\xi_{k,+}\xi_{m',+}^*\xi_{n',+}\xi_{k',+}^*\right\}, \\ \times\mathrm{E}\left\{\xi_{m,+}\xi_{n,+}^*\xi_{k,+}\xi_{m',-}^*\xi_{n',-}\xi_{k',+}^*\right\} \\ \mathrm{E}\left\{\xi_{m,-}\xi_{n,-}^*\xi_{k,+}\xi_{m',+}^*\xi_{n',+}\xi_{k',+}^*\right\}, \\ \times\mathrm{E}\left\{\xi_{m,-}\xi_{n,-}^*\xi_{k,+}\xi_{m',-}^*\xi_{n',-}\xi_{k',+}^*\right\} \end{bmatrix} \quad (24)$$

In (24), the arrays (m,n,k) and (m',n',k') are both included in the subset A_i. Each term in set (24) follows a similar calculation process. Let's take the first term as an example to illustrate

the calculation process. First, we divide the 6 random variables in the first term of the expectation into two categories based on whether they are complex conjugates. Our goal is to pair these random variables into three pairs of random variables multiplied by their modulus squared. Otherwise, according to (23), their contribution to the mean will be zero. Considering the constraint of subset v (i.e.,$m,k\neq n$ and $m',k'\neq n'$), we can proceed as follows, as shown in Fig. 2:

- In the first step, $\xi_{n',+}$ can only be paired with $\xi_{n,+}^*$.
- In the second step, $\xi_{m,+}^*$ can be paired with either $\xi_{m',+}$ or $\xi_{k',+}^*$.
- In the third step, we pair the remaining two random variables.

Based on the analysis above, the first term of the expectation in set (24) equals 2. Other expectation terms can be calculated using the same approach.

Here is the final result:

$$\begin{bmatrix} \mathrm{E}\left\{\xi_{m,+}\xi_{n,+}^*\xi_{k,+}\xi_{m',+}^*\xi_{n',+}\xi_{k',+}^*\right\},\mathrm{E} \\ \times\left\{\xi_{m,+}\xi_{n,+}^*\xi_{k,+}\xi_{m',-}^*\xi_{n',-}\xi_{k',+}^*\right\} \\ \mathrm{E}\left\{\xi_{m,-}\xi_{n,-}^*\xi_{k,+}\xi_{m',+}^*\xi_{n',+}\xi_{k',+}^*\right\},\mathrm{E} \\ \times\left\{\xi_{m,-}\xi_{n,-}^*\xi_{k,+}\xi_{m',-}^*\xi_{n',-}\xi_{k',+}^*\right\} \end{bmatrix} = \begin{bmatrix} 2,0 \\ 0,1 \end{bmatrix} \quad (25)$$

Substituting the above result into (22) and simplifying, the average power spectral density of nonlinear crosstalk in a same-wavelength bidirectional scenario can be expressed as:

$$G_{NLI}(z,f) = \gamma^2 p_+(z)\times$$

$$\begin{Bmatrix} 2\times\int_{-\infty}^{+\infty}\int_{-\infty}^{+\infty}G_{Tx}(f_1)G_{Tx}(f_2)G_{Tx}(f_1+f_2-f) \\ \rho_+(z,f)\,df_1df_2+ \\ 1\times\int_{-\infty}^{+\infty}\int_{-\infty}^{+\infty}G_{Tx}(f_1)G_{Tx}(f_2)G_{Tx}(f_1+f_2-f) \\ \rho_-(z,f)\,df_1df_2 \end{Bmatrix}$$

$$(26)$$

Where $\rho_+(z,f)$ and $\rho_-(z,f)$ represent the four-wave mixing (FWM) efficiencies for the forward and backward transmission of signal light, respectively, and they are defined as:

$$\begin{cases} \rho_+(z,f) = \left|\int_0^z p_+(\sigma)e^{j4\pi^2\beta_2(f_1-f)(f_2-f)\sigma}d\sigma\right|^2 \\ \rho_-(z,f) = \left|\int_0^z \frac{p_-(0)}{p_-(L-\sigma)}\right. \\ \left.\times e^{j\{[4\pi^2\beta_2(f_1+f_2)(f_2-f)+4\pi\beta_1(f_2-f)]\sigma\}}d\sigma\right|^2 \end{cases} \quad (27)$$

Where β_1 and β_2 are derived from the first and second derivatives of the propagation constant β using a Taylor series expansion.

Equation (27) consists of two terms. The first term is identical to the expression of the GN model in a unidirectional transmission system under the single-polarization condition [25]. The second term represents additional nonlinear interference introduced by the opposite-end signal.

III. DISCUSSIONS OF THE NONLINEAR INTERFERENCE MODEL

According to (26), if the integral values of the two terms in the equation are equal, the ratio of NLI introduced by the
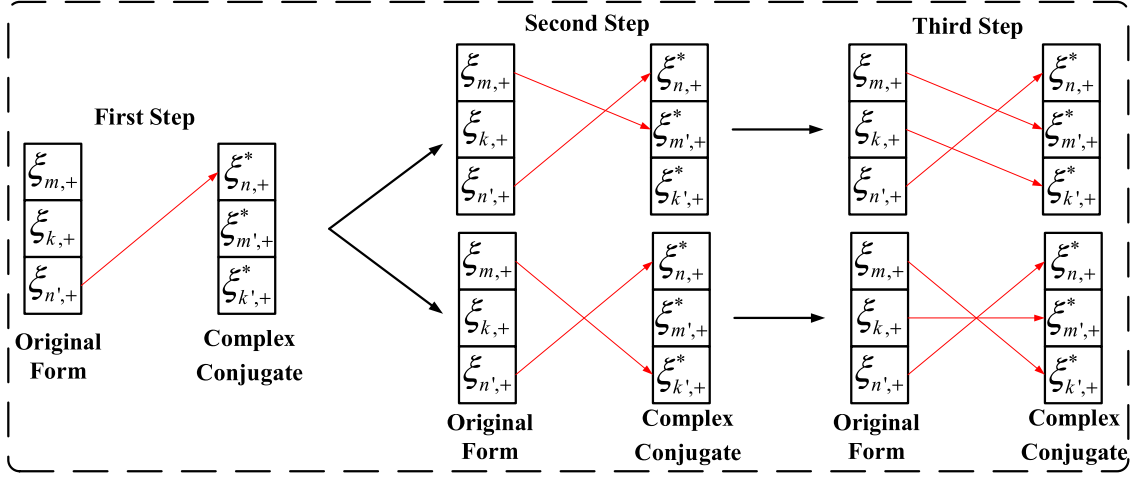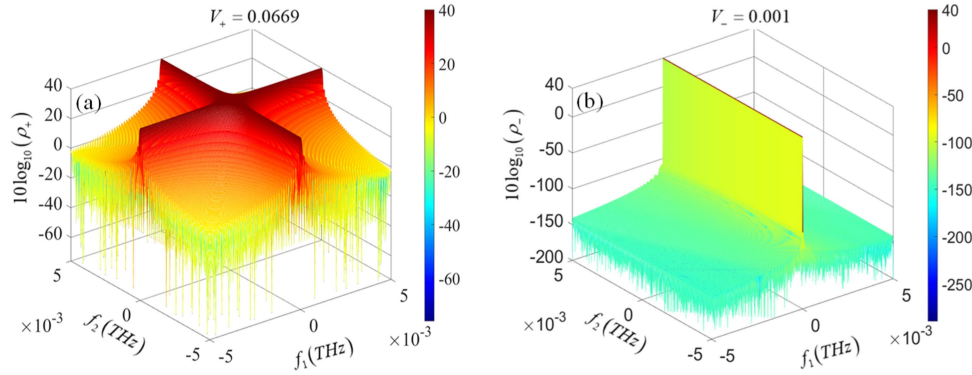
Fig. 2. Calculation process of the expectations.

Fig. 3. Distribution of FWM efficiency in the $f_1 - f_2 - \rho$ space: (a) $\rho_+(z, f)$; (b) $\rho_-(z, f)$.

forward and backward signals is 2:1. However, in reality, the contributions of the forward and backward signals will strongly depend on their respective FWM efficiencies. For analytical convenience, in (26), we remove the coefficients associated with the normalized power characteristics. Additionally, considering that the two integrals have a similar functional form, this set of equations can be written in a unified form as follows:

$$\rho(z, f) = \left| \int_0^z e^{jk\sigma} d\sigma \right|^2 = \frac{2 - 2\cos(kz)}{k^2} \quad (28)$$

Where setting $k = 4\pi^2 \beta_2 (f_1 - f)(f_2 - f)$ corresponding to $\rho_+(z, f)$ and setting $k = [4\pi^2 \beta_2 (f_2 + f_1) + 4\pi\beta_1](f_2 - f)$ allows us to obtain $\rho_-(z, f)$.

Obviously, as k approaches zero, (28) will attain its maximum value, which can be expressed as follows:

$$\rho_{\max} = \lim_{k \to 0} \frac{2 - 2\cos(kz)}{k^2} = z^2 \quad (29)$$

Equation (29) indicates that ρ_+ reaches its maximum value when $f_1 = f$ or $f_2 = f$, while ρ_- reaches its maximum value when $f_2 = f$, and both maximum values are equal to z^2. As k gradually moves away from zero, the FWM efficiencies decay rapidly at a rate of $1/k^2$. Therefore, it can be inferred that ρ_+

TABLE I
SIMULATION PARAMETERS FOR FWM EFFICIENCY

z(km)	f(THz)	β_1(ps/km)	β_2(ps²/km)	Frequency Range
100	0	3.3×10^6	-24	$[-5,5] \times 10^{-3}$

and ρ_- only contribute to the double integral in (26) within a small region near their respective maximum points.

To illustrate this phenomenon more intuitively, we provide the three-dimensional function distribution plot of ρ_+ and ρ_- on the space $f_1 - f_2 - \rho$ in a specific case, as shown in Fig. 3. The simulation parameters are provided in Table I.

The simulation results in Fig. 3 are consistent with our expectations. For ρ_+, its values are mainly concentrated near the plane $f_1 = f$ and plane $f_2 = f$, and they decay rapidly with a rate of $1/(4\pi^2 \beta_2 f_1 f_2)^2$ in all directions. In addition, the values of ρ_- are primarily concentrated near the plane $f_2 = f$, and they decay with a rate of $1/\{[4\pi^2 \beta_2 (f_2 + f_1) + 4\pi\beta_1] f_2\}^2$. It is noteworthy that for ρ_- the main contribution to this decay rate comes from the term $4\pi\beta_1 f_2$, which is caused by the strong walk-off effect introduced by the signals propagating in opposite directions. This results in an extremely steep downward trend.
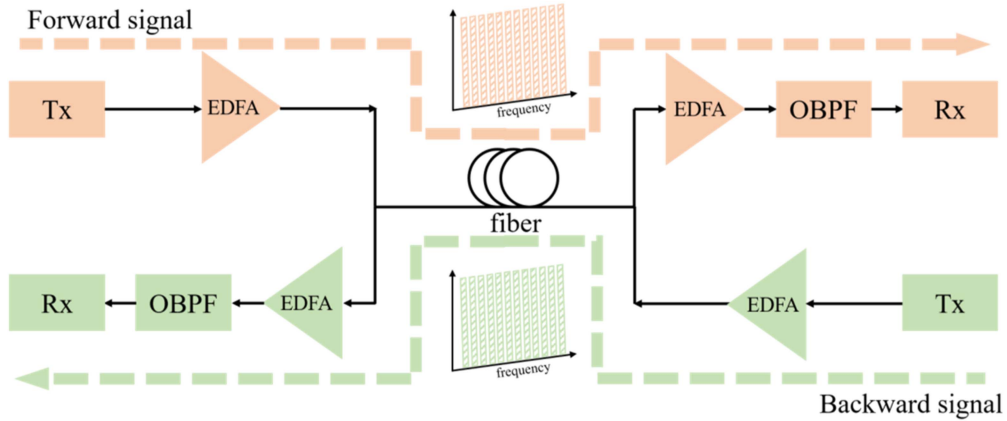
Fig. 4. Simulation link structure diagram of a same-wavelength bidirectional coherent optical fiber communication system.

TABLE II
SIMULATION SYSTEM PARAMETERS CONFIGURATION

Parameters	Value
Modulation Format	16 QAM
Baud Rate	32 Gbaud
Sequence Length	65536
Samples Per Bit	4
Wavelength	1550 nm
Noise Figure for EDFA	4 dB
Fiber Length	75/100/120 km
Bandwidth of the optical filter	50 GHz

For the double integral shown in (26), under the influence of the decay of ρ_-, the effective integration domain of the second term will collapse into a "line." Under this condition, its contribution to the integral value is almost zero.

More specifically, we can approximate the contribution of NLI by considering the volume of ρ_+ and ρ_- on the three-dimensional space of $f_1 - f_2 - \rho$. The volumes of ρ_+ and ρ_- are denoted as $V_+ = 0.0669$ and $V_- = 0.001$, respectively. If we consider the integral coefficients in (26), the ratio of NLI introduced by the forward and backward transmitted signal light can be expressed as $10\log_{10}(2V_+/V_-) \approx 21dB$. Therefore, it can be theoretically deduced that the backward signal does not induce significant NLI on the forward signal.

IV. SIMULATION VERIFICATION OF THE NONLINEAR INTERFERENCE MODEL

In the previous section, we derived the conclusion from a theoretical perspective that in a same-wavelength bidirectional coherent optical communication system, the backward signal does not impose additional nonlinear interference on the forward signal. To validate this conclusion at the system level, in this section, we have constructed a simulation platform for a SWB coherent optical fiber communication system based on Optisystem software. The system block diagram is depicted in Fig. 4, and the simulation parameters are detailed in Table II.

During the simulation process, we modulated both the forward and backward transmitted signals with 32 Gbaud DP-16QAM

signals. The modulated signals were then adjusted in power using a pre-amplifier (PA) and fed into the bidirectional fiber transmission module. To compensate for the losses in the fiber link, the transmitted signal power was amplified using a booster amplifier (BA). Subsequently, the optical signal was filtered and coherent reception was performed. The received signal was processed through DSP to obtain the constellation diagram of the electrical signal. From the constellation diagram, the corresponding error vector magnitude (EVM) was derived, which served as the evaluation metric for signal transmission quality. It should be noted that in the simulation, we have set the Rayleigh scattering effect in the bidirectional fiber transmission module to be disabled. Under this condition, the additional factors that may affect signal transmission quality are primarily the nonlinear interference. Therefore, the validity of the aforementioned conclusion can be verified by comparing and analyzing the signal quality between unidirectional transmission and bidirectional transmission scenarios.

To demonstrate the generalizability of the simulation, we conducted tests at three different transmission distances: 80 km, 100 km, and 120 km. We investigated the relationship between the input fiber power and the error vector magnitude (EVM). EVM can be calculated through this formula:

$$EVM = 10 * \log 10 \left(\left(\sum_{i=1}^{n} |xout(i) - xin(i)|^2 \right) / n \right) \tag{30}$$

Where x_{out} and x_{in} represent the normalized signal sequence at the receiving and originating ends.

The results of these tests are shown in Fig. 5. It can be observed that as the input power increases, the signal quality is initially optimized due to the improvement in input optical signal-to-noise ratio (OSNR), resulting in a decrease in EVM. However, as the input power continues to increase, nonlinear effects in the fiber gradually accumulate, leading to an increase in EVM. Importantly, under both unidirectional and bidirectional transmission conditions, the EVM curves almost completely overlap, indicating that the nonlinear effects from the backward direction do not further degrade the signal quality of the forward
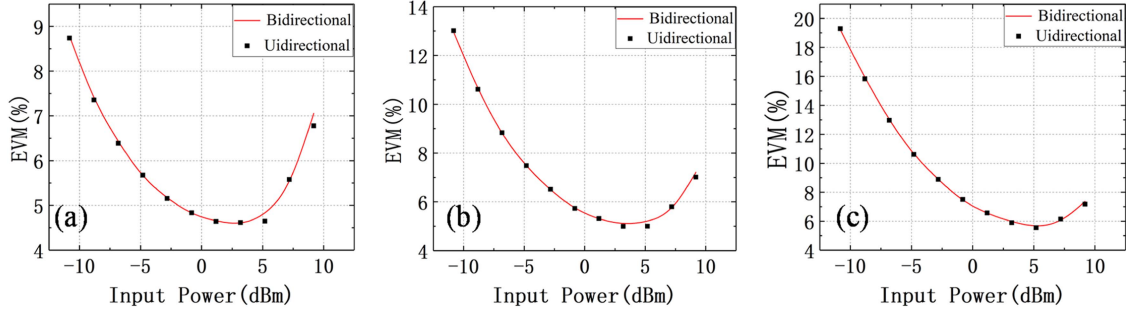
Fig. 5. Relationship curve between EVM and input fiber power: (a) 80 km; (b) 100 km; (c) 120 km.

signal. This confirms the validity of our conclusion in this simulated transmission system.

V. CONCLUSION

In this article, we conduct thorough theoretical research on nonlinear interference in same-wavelength bidirectional coherent optical communication systems. The traditional GN model which is used to evaluate NLI in traditional unidirectional systems is extended to the bidirectional transmission scenario. After analyzing and discussing the extended nonlinear model, we arrive at an important conclusion: in a bidirectional transmission communication system, due to the strong walk-off effect between forward and backward transmitted signals, the backward signal almost does not introduce additional nonlinear crosstalk to the forward signal.

Specifically, the ratio of the nonlinear crosstalk introduced by the forward and backward signals is about 21 dB, indicating that the system's tolerance to NLI is nearly the same as that of traditional unidirectional systems. Therefore, the traditional GN model is applicable in the bidirectional scenario as well. Furthermore, we built a simulation platform based on Optisystem software. In scenarios with transmission distances of 80/100/120 km, we compared the received signal's EVM in both unidirectional and bidirectional transmission systems. The results show that the EVM curves of both scenarios completely overlap, confirming the validity of the aforementioned conclusion.

APPENDIX

The derivation of the pulse transmission equation in the single fiber bidirectional scenario also needs to start from Maxwell's equations. The corresponding wave equation can be obtained after electromagnetic separation:

$$\nabla^2 \vec{E} = \mu_0 \varepsilon_0 \frac{\partial^2 \vec{E}}{\partial t^2} + \mu_0 \frac{\partial^2 \left(\vec{P}_L + \vec{P}_{NL} \right)}{\partial t^2} \tag{31}$$

Where $\vec{E}$ is the electric field intensity of the optical signal. $\vec{P}_L$ and $\vec{P}_{NL}$ are linear and nonlinear parts of induced polarization intensity respectively. μ_0 and ε_0 are the dielectric constant and permeability in vacuum.

Generally speaking, the frequency of the modulation signal on the optical field is much lower than the optical frequency. In this context, the slow variable envelope approximation can be adopted to separate the fast variable part of the electric field and

polarization intensity that vibrates with the optical frequency and writen as follows:

$$\begin{cases} 2\vec{E} = [E_+ \left(\vec{r}, t \right) \exp \left(-i\omega_0 t \right) \\ \quad + E_- \left(\vec{r}, t \right) \exp \left(-i\omega_0 t \right) + c.c] \\ 2\vec{P}_L = [P_L \left(\vec{r}, t \right) \exp \left(-i\omega_0 t \right) + c.c] \\ 2\vec{P}_{NL} = [P_{NL} \left(\vec{r}, t \right) \exp \left(-i\omega_0 t \right) + c.c] \end{cases} \tag{32}$$

Where E_+ and E_- represent the time slowing-change function of forward and backward transmission optical fields respectively. P_L and P_{NL} is the slow-changing part corresponding to the polarization intensity. The light field and polarization intensity can be related by polarizability χ, and the relationship between the two can be given by the following formula when only polarization x is considered:

$$\begin{cases} \vec{P}_L = \frac{1}{2}\varepsilon_0\chi_{xx}^{(1)} \left[(E_+ \left(\vec{r}, t \right) + E_- \left(\vec{r}, t \right)) \exp \left(-i\omega_0 t \right) + c.c \right] \\ \vec{P}_{NL} = \frac{3}{8}\varepsilon_0\chi_{xxxx}^{(3)} \left[|E_+ + E_-|^2 \left(E_+ + E_- \right) \right. \\ \left. \quad \times \exp \left(-i\omega_0 t \right) + c.c \right] \end{cases} \tag{33}$$

By comparing (32) and (33), it is easy to obtain the expression of the slow-changing part of the polarization intensity, as shown below:

$$\begin{cases} P_L = \varepsilon_0\chi_{xx}^{(1)} \left[E_+ \left(\vec{r}, t \right) + E_- \left(\vec{r}, t \right) \right] \\ P_{NL} = \varepsilon_0\varepsilon_{NL} \left[E_+ \left(\vec{r}, t \right) + E_- \left(\vec{r}, t \right) \right] \end{cases} \tag{34}$$

Where $\varepsilon_{NL} = \frac{3}{4}\chi_{xxxx}^{(3)}|E_+ + E_-|^2\circ$

Equation (31) is more convenient to deal with in the frequency domain, where the time differential operator $\frac{\partial}{\partial t}$ can be directly repla0ced by $-i\omega_0$, so the time derivative part can be removed. Therefore, we do the Fourier transform on both ends of (31), and substitute (32) into it, and get:

$$\nabla^2 \left[E_+ \left(\omega - \omega_0 \right) + E_- \left(\omega - \omega_0 \right) \right]$$
$$= -\omega^2\mu_0\varepsilon_0 \left[E_+ \left(\omega - \omega_0 \right) + E_- \left(\omega - \omega_0 \right) \right]$$
$$- \omega^2\mu_0 \left[P_L \left(\omega - \omega_0 \right) + P_{NL} \left(\omega - \omega_0 \right) \right] \tag{35}$$

After transforming (34) into the frequency domain and substituting it into (35) and sorting it out, the corresponding Helmholtz equation can be obtained, as shown in (36) :

$$\nabla^2 \left[E_+ \left(\omega - \omega_0 \right) + E_- \left(\omega - \omega_0 \right) \right]$$
$$+ \varepsilon \left(\omega \right) k_0^2 \left[E_+ \left(\omega - \omega_0 \right) + E_- \left(\omega - \omega_0 \right) \right] = 0 \tag{36}$$

In the formula, the corrected dielectric constant is $\varepsilon(\omega) = 1 + \tilde{\chi}_{xx}^{(1)}(\omega) + \varepsilon_{NL}(\omega)$, and $k_0 = \frac{\omega}{c}$.

Similar to the derivation of the pulse transmission equation under unidirectional transmission, the solution of (36) can also adopt the separation variable method, in which we assume that the tentative solutions of the forward and backward transmitted light meet the following forms respectively:

$$
\begin{cases}
E_+ \left(\omega - \omega_0 \right) = F_+ \left(x, y \right) \tilde{A}_+ \left(z, \omega - \omega_0 \right) \exp \left(i\beta_0 z \right) \\
E_- \left(\omega - \omega_0 \right) = F_- \left(x, y \right) \tilde{A}_- \left(z, \omega - \omega_0 \right) \\
\qquad \times \exp \left[i\beta_0 \left(L - z \right) \right]
\end{cases}
\tag{37}
$$

The transverse component of the light field is described by $F(x,y)$ in the formula. The slow variable envelope of longitudinal transmission is characterized by $\tilde{A}(z, \omega - \omega_0)$. $\beta_0 = \beta(\omega_0)$ and L represent wave number and fiber length, respectively.

Equation (37) is substituted into Helmholtz equation and separated according to longitudinal and transverse components. The pulse transmission equation describing signal transmission in the frequency domain can be obtained and is shown in (38):

$$
\begin{cases}
\frac{\partial \tilde{A}_+}{\partial z} = i \left[\beta \left(\omega \right) + \Delta\beta \left(\omega \right) - \beta_0 \right] \tilde{A}_+ = 0 \\
\frac{\partial \tilde{A}_-}{\partial z} - i \left[\beta \left(\omega \right) + \Delta\beta \left(\omega \right) - \beta_0 \right] \tilde{A}_- = 0
\end{cases}
\tag{38}
$$

Where $\Delta\beta(\omega) = \gamma |E_+ + E_-|^2$ can be obtained by the first-order perturbation theory, in which γ is the nonlinear coefficient of the fiber. The inverse Fourier transformation of the above equation can obtain the transmission equation of $A_+(z,t)$ and $A_-(z,t)$ in the time domain, but it is usually difficult to obtain the specific form of wave number $\beta(\omega)$, thus we consider the Taylor series expansion near the optical frequency ω_0:

$$
\beta \left(\omega \right) = \sum_{n=1}^{\infty} \frac{\left(\omega - \omega_0 \right)^n}{n!} \left(\frac{d^n \beta}{d\omega^m} \right)_{\omega = \omega_0}
\tag{39}
$$

Equation (39) is substituted into (38), and inverse Fourier transformation is performed on both sides of the equation at the same time. In this process, $(\omega - \omega_0)$ can be replaced by differential operator $(i\partial/\partial t)$. Here, we only consider the influence of second-order dispersion. Finally, the pulse transmission equation in the time domain can be written as follows:

$$
\begin{cases}
\frac{\partial A_+}{\partial z} + \beta_1 \frac{\partial A_+}{\partial t} + \frac{i\beta_2}{2} \frac{\partial^2 A_+}{\partial t^2} = i\gamma \\
\qquad \times \left(\begin{array}{c} |A_+|^2 + |A_-|^2 + A_+^* A_- \exp \left[i\beta_0 \left(L - 2z \right) \right] \\ + A_+^* A_- \exp \left[-i\beta_0 \left(L - 2z \right) \right] \end{array} \right) A_+ \\
\frac{\partial A_-}{\partial z} - \beta_1 \frac{\partial A_-}{\partial t} - \frac{i\beta_2}{2} \frac{\partial^2 A_-}{\partial t^2} = -i\gamma \\
\qquad \times \left(\begin{array}{c} |A_+|^2 + |A_-|^2 + A_-^* A_+ \exp \left[i\beta_0 \left(L - 2z \right) \right] \\ + A_-^* A_+ \exp \left[-i\beta_0 \left(L - 2z \right) \right] \end{array} \right) A_-
\end{cases}
\tag{40}
$$

Note that the last two terms of the above equations are related to the correlation coupling between the former and post-transmitted signals, and their importance depends on the degree of phase matching satisfaction. For the case of long-distance transmission, the average effect is zero, so the above equation can be simplified as:

$$
\begin{cases}
\frac{\partial A_+}{\partial z} + \beta_1 \frac{\partial A_+}{\partial t} + \frac{i\beta_2}{2} \frac{\partial^2 A_+}{\partial t^2} = i\gamma \left(|A_+|^2 + |A_-|^2 \right) A_+ \\
\frac{\partial A_-}{\partial z} - \beta_1 \frac{\partial A_-}{\partial t} - \frac{i\beta_2}{2} \frac{\partial^2 A_-}{\partial t^2} = -i\gamma \left(|A_+|^2 + |A_-|^2 \right) A_-
\end{cases}
\tag{41}
$$

In order to reach agreement with the signal model in terms of expression, we uniformly rewrite $A_\pm(z,t)$ in the pulse transmission equation described in (41) into $E_\pm(z,t)$, and retain the original form of its wave number $\beta(\omega)$, and then we do Fourier transform at both ends of the equation at the same time to obtain:

$$
\begin{cases}
\frac{\partial}{\partial z} E_+ \left(z, f \right) = -j\beta \left(f \right) E_+ \left(z, f \right) + \left[-\alpha + g \left(z \right) \right] \\
\qquad \times E_+ \left(z, f \right) + Q_{NLI,+} \\
\frac{\partial}{\partial z} E_- \left(z, f \right) = +j\beta \left(f \right) E_- \left(z, f \right) - \left[-\alpha + g \left(z \right) \right] \\
\qquad \times E_- \left(z, f \right) + Q_{NLI,-}
\end{cases}
\tag{42}
$$

$Q_{NLI,\pm}(z,f)$ is the nonlinear Kerr term, which is obtained by transforming the right side of Formula (41) and can be expressed as:

$$
\begin{cases}
Q_{NLI,+} \left(z, f \right) = -j\gamma \left[E_+ \left(z, f \right) * E_+^* \left(z, f \right) \right. \\
\qquad \left. + E_- \left(z, f \right) * E_-^* \left(z, f \right) \right] * E_+ \left(z, f \right) \\
Q_{NLI,-} \left(z, f \right) = +j\gamma \left[E_+ \left(z, f \right) * E_+^* \left(z, f \right) \right. \\
\qquad \left. + E_- \left(z, f \right) * E_-^* \left(z, f \right) \right] * E_- \left(z, f \right)
\end{cases}
\tag{43}
$$

Where "$*$" stands for convolution operation.

REFERENCES

[1] J. W. Peter, T. N. David, and R. C. Andrew, "Fiber-optic transmission and networking: The previous 20 and the next 20 years," *Opt. Exp.*, vol. 26, pp. 24190–24239, Aug. 2018, doi: 10.1364/OE.26.024190.

[2] C. K. Daniel and P. Nasser, "Changing evolution of optical communication systems at the network edges," *Appl. Opt.*, vol. 59, pp. G209–G218, Jul. 2020, doi: 10.1364/AO.394119.

[3] T. Mizuno, H. Takara, A. Sano, and Y. Miyamoto, "Dense space-division multiplexed transmission systems using multi-core and multi-mode fiber," *J. Lightw. Technol.*, vol. 34, no. 2, pp. 582–592, Jan. 2016, doi: 10.1109/JLT.2015.2482901.

[4] D. J. Richardson, J. M. Fini, and L. E. Nelson, "Space-division multiplexing in optical fibres," *Nature Photon.*, vol. 7, pp. 354–362, Apr. 2013, doi: 10.1038/nphoton.2013.94.

[5] L.-S. Yan, X. Liu, and W. Shieh, "Toward the Shannon limit of spectral efficiency," *IEEE Photon. J.*, vol. 3, no. 2, pp. 325–330, Apr. 2011, doi: 10.1109/JPHOT.2011.2127468.

[6] Y. Chiniforooshan, X. Tang, Z. Jiang, and Z. Zhang, "High capacity coherent systems using same-wavelength bidirectional transmission," in *Proc. Asia Commun. Photon. Conf.*, 2019, pp. 1–3.

[7] W. Yu, H. Shi, Y. Liu, W. Shang, Y. Jia, and Z. Feng, "Experimental demonstration of 160 × 100Gb/s real-time WDM bidi-transmission over 100-km G.652 fiber," in *Proc. Asia Commun. Photon. Conf.*, 2021, pp. 1–3.

[8] E. Virgillito et al., "Propagation impairment in single-wavelength, single-fiber bidirectional optical transmission," in *Proc. Optica Adv. Photon. Congr.*, 2022, pp. NeTu3D–3.

[9] J. Ko, S. Kim, J. Lee, S. Won, Y. S. Kim, and J. Jeong, "Estimation of performance degradation of bidirectional WDM transmission systems due to Rayleigh backscattering and ASE noises using numerical and analytical models," *J. Lightw. Technol.*, vol. 21, no. 4, pp. 938–946, Apr. 2003, doi: 10.1109/JLT.2003.810086.

[10] M. Xu, Z. Jia, J. Zhang, H. Zhang, and L. A. Campos, "Efficient echo-cancellation algorithms for full duplex coherent optical systems," in *Proc. Opt. Fiber Commun. Conf. Exhib.*, 2020, pp. 1–3.

[11] Y. Wang and W. Li, "LFMTS-assisted reflection interference elimination method for a coherent same-wavelength bidirectional optical communication system," *Opt. Exp.*, vol. 29, no. 13, pp. 20077–20091, 2021, doi: 10.1364/OE.430293.

[12] Y. Wang et al., "Demonstrations of 160×28 GBaud C-band same-wavelength bidirectional fiber transmission experiments," in *Proc. Conf. Lasers Electro-Opt.*, 2022, pp. 1–2.

[13] C. Wu et al., "110.4 Tbit/s same-wavelength bidirectional optical fiber transmission over 100 km G. 654D Fiber in super-C band with rayleigh scattering noise suppressed by Raman amplifiers," in *Proc. Opt. Fiber Commun. Conf. Exhib.*, 2023, pp. 1–3.

[14] G. P. Agrawal, *Nonlinear Fiber Optics*, 5th ed. New York, NY, USA: Academic, 2012.

[15] P. Poggiolini, "The GN model of non-linear propagation in uncompensated coherent optical systems," *J. Lightw. Technol.*, vol. 30, no. 24, pp. 3857–3879, Dec. 2012.

[16] J. Zhou, J. Lu, C. Lu, and C. Yu, "The impact of parameter uncertainty on QoT estimation using GN-based analytical model," in *Proc. 26th Optoelectron. Commun. Conf.*, 2021, pp. M4A.2.

[17] J. Lu et al., "Performance comparisons between machine learning and analytical models for quality of transmission estimation in wavelength-division-multiplexed systems," *J. Opt. Commun. Netw.*, vol. 13, no. 4, pp. B35–B44, Jan. 2021, doi: 10.1364/JOCN.410876.

[18] Y. Xu, L. Yan, E. Agrell, and M. B. Pearce, "Iterative resource allocation algorithm for EONs based on a linearized GN model," *J. Opt. Commun. Netw.*, vol. 11, no. 3, pp. 39–51, Jan. 2019, doi: 10.1364/JOCN.11.000039.

[19] A. Gafur, M. R. Ahmed, A. R. Md Foisal, and M. Badiuzzaman, "OSNR improvement of coherent uncompensated optical transmission systems for various commercial optical fiber types," in *Proc. Int. Conf. Elect. Eng. Inf. Commun. Technol.*, 2014, pp. 1–5, doi: 10.1109/ICEEICT.2014.6919079.

[20] A. Mecozzi and R.-J. Essiambre, "Nonlinear Shannon limit in pseudolinear coherent systems," *J. Lightw. Technol.*, vol. 30, no. 12, pp. 2011–2024, Jun. 2012, doi: 10.1109/JLT.2012.2190582.

[21] R. Dar, M. Feder, A. Mecozzi, and M. Shtaif, "Inter-channel nonlinear interference noise in WDM systems: Modeling and mitigation," *J. Lightw. Technol.*, vol. 33, no. 5, pp. 1044–1053, Mar. 2015, doi: 10.1109/JLT.2014.2384998.

[22] P. Poggiolini, G. Bosco, A. Carena, V. Curri, Y. Jiang, and F. Forghieri, "The GN-model of fiber non-linear propagation and its applications," *J. Lightw. Technol.*, vol. 32, no. 4, pp. 694–721, Feb. 2014, doi: 10.1109/JLT.2013.2295208.

[23] A. Carena, V. Curri, G. Bosco, P. Poggiolini, and F. Forghieri, "Modeling of the impact of nonlinear propagation effects in uncompensated optical coherent transmission links," *J. Lightw. Technol.*, vol. 30, no. 10, pp. 1524–1539, May 2012, doi: 10.1109/JLT.2012.2189198.

[24] V. Curri, A. Carena, P. Poggiolini, G. Bosco, and F. Forghieri, "Extension and validation of the GN model for non-linear interference to uncompensated links using Raman amplification," *Opt. Exp.*, vol. 21, no. 3, pp. 3308–3317, Feb. 2013, doi: 10.1364/OE.21.003308.

[25] P. Poggiolini, G. Bosco, A. Carena, V. Curri, Y. Jiang, and F. Forghieri, "A detailed analytical derivation of the GN model of non-linear interference in coherent optical transmission systems," *Physics*, 2012, doi: 10.48550/arXiv.1209.0394.